HELIUM I λ10830 AS A PROBE OF MAGNETOSPHERIC ACCRETION.

W. J. Fischer, *Five College Astronomy, University of Massachusetts, Amherst MA 01003, USA, (wfischer@astro.umass.edu)*, S. Edwards, *Five College Astronomy, Smith College, Northampton MA 01063, USA*, J. Kwan, *Five College Astronomy, University of Massachusetts, Amherst MA 01003, USA*, L. Hillenbrand, *Department of Astronomy, California Institute of Technology, Pasadena CA 91125, USA*.

He I λ10830 profiles of 38 CTTS spanning three orders of magnitude in mass accretion rate were extracted from one-micron spectra obtained with NIRSPEC on Keck II. Edwards et al. (2006) found that 89% of this sample shows subcontinuum absorption at λ10830, where 71% show blueshifted absorption from a wind, and 53% show redshifted absorption. Figure 1 displays profiles of the 20 CTTS with redshifted subcontinuum absorption, ordered from top to bottom by increasing red absorption equivalent width, which ranges from 0.2 to 4.5 Å. The observed absorptions are often deep, with depths ranging from 8 to 61% of the continuum, and wide, with widths ranging from 80 to 390 km s^{-1}. The frequency of redshifted subcontinuum absorption at λ10830 is higher for stars with low one-micron veilings r_Y: Among the 30 stars with $r_Y < 0.5$, 19 (63%) show red absorption. In contrast, only 1 of the 8 stars with $r_Y \geq 0.5$ shows red absorption.

The He I λ10830 transition ($2p\,^3P^o \rightarrow 2s\,^3S$) is a powerful probe of the star-disk interaction. The location of the lower level 21 eV above the ground state restricts line formation to regions of high temperature or high ionizing photon flux, as expected in the innermost few stellar radii. The high frequency of absorption in this line arises from the metastability of the lower level. Further, since the only permitted transition from the upper level is emission of a λ10830 photon, this line can be modeled with simple resonance scattering. When the absorption is located blueward of line center, it can be used to distinguish among wind-launching geometries. Kwan et al. (2007) found evidence for both a disk wind and an accretion-powered stellar wind in their study of blue absorption components.

When the absorption is located redward of line center, it tracks the geometry of the accretion flow from the disk to the star. Under the assumption of single scattering, the depth of the absorption at each velocity maps the percentage of the stellar surface occulted at that velocity. Our data imply that the accretion flow can obscure up to 40% of the visible surface of the star over a velocity interval of 100 km s^{-1} and up to 20% of the visible surface over a velocity interval of 200 km s^{-1}. In the standard model, the accretion flow is assumed to occur along stellar dipole field lines that intersect the disk, guiding material in free-fall toward the star (Hartmann et al. 1994). By simulating resonance scattering in dipole field geometries of various sizes, we calculate model helium profiles and compare them to the observations. The scattering assumption gives us new insight into the infall geometry without a detailed understanding of the temperature of the flow, a noted challenge in existing radiative transfer models (Muzerolle et al. 2001).

We characterize the dipole geometry with two parameters: (1) a fiducial disk interaction radius R_0, which defines the radius in the disk from which the flow originates, and (2) a filling factor f, which is the fraction of the stellar surface

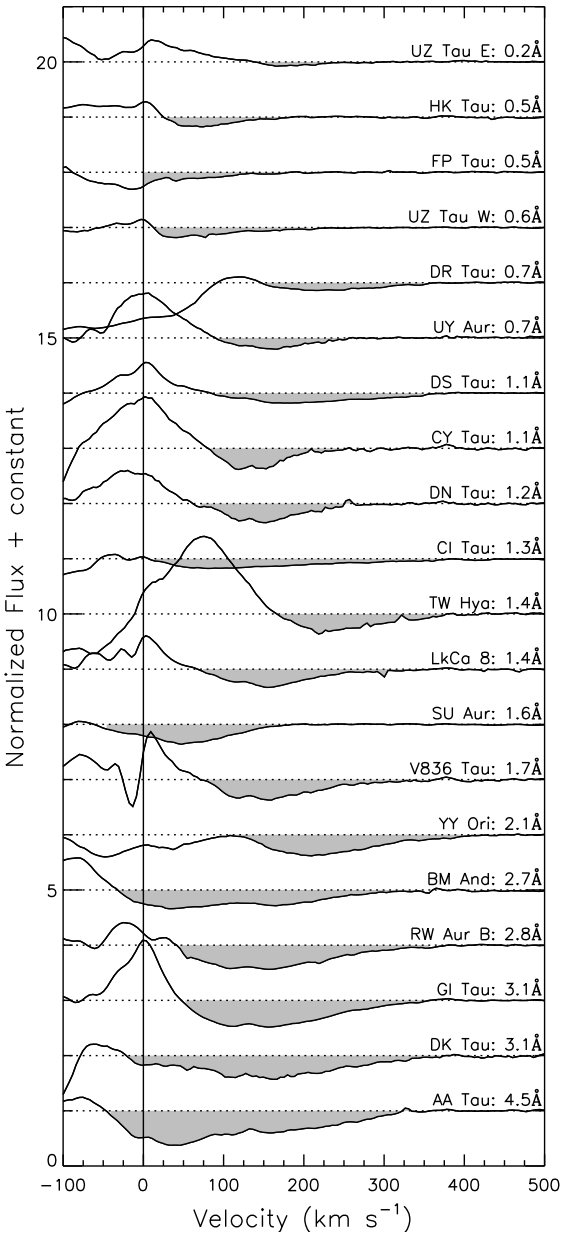

Figure 1: He I λ10830 profiles for the 20 of 38 CTTS with subcontinuum redshifted absorption. The profiles are ordered from top to bottom by increasing red absorption equivalent width, shown on the right side of the figure. Photospheric features have been subtracted from the profiles, and zero velocity represents rest relative to the photosphere.

intercepted by accreting field lines. Together these parameters specify a unique flow. We explore fiducial disk interaction radii from $R_0 = 2$ to 8 R_*, typical of co-rotation radii, and filling factors from $f = 1$ to 10%, typical of those found by modeling the luminosity attributed to accretion shocks on the stellar surface (Calvet & Gullbring 1998). The velocity law includes components due to free-fall and rotation of the magnetosphere.

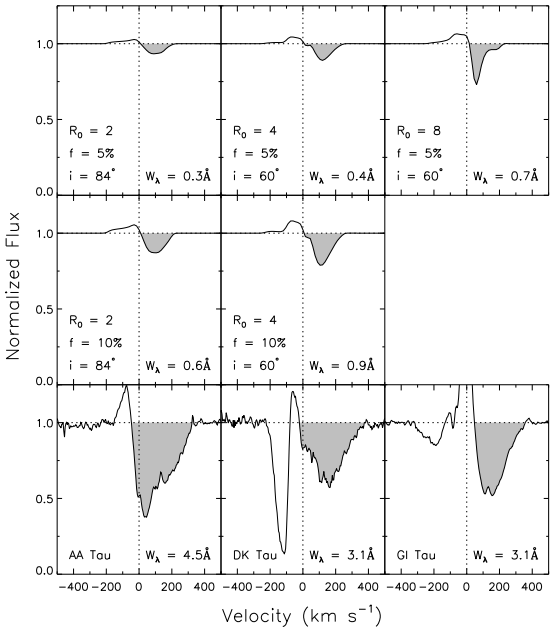

Figure 2: Model He I λ10830 scattering profiles with the strongest red absorptions (top two rows) compared to the three observed profiles with the strongest red absorptions (bottom row). The model profiles are those with the largest red absorptions from each of the five geometries with photospheric filling factor greater than 1%.

We find that these plausible dipole geometries are insufficient to reproduce the red absorption morphologies of 70% of the observed profiles. Although filling factors inferred from accretion shock luminosities are about 1% for many CTTS (Calvet & Gullbring 1998), we find that filling factors of 1% yield red absorption equivalent widths of at most 0.2 Å. In contrast, only 1 of the 20 observed profiles has a red absorption equivalent width this small. Even with filling factors of 5 and 10%, the maximum equivalent width among the model profiles is 0.9 Å. Only 6 of the 20 observed profiles have red absorption equivalent widths smaller than this. This is illustrated in Figure 2, where the top two rows show model profiles for filling factors of 5 and 10% at the inclination angles with the strongest absorptions. The bottom row shows observed profiles for the stars with the three strongest red absorptions. As seen in the figure, the deepest and widest model profiles never absorb more than 20% of the continuum over a range of more than 50 km s^{-1}, in strong contrast to the majority of the observed profiles. Two possible effects that could account for the inferred deviations from an axisymmetric dipole flow are misaligned dipoles coupled with disk warping (Bouvier et al. 1999, Romanova et al. 2003) or flows that have large radial components (Gregory et al. 2006).

REFERENCES

Bouvier, J., et al. 1999, A&A, 349, 619
Calvet N., & Gullbring, E. 1998, ApJ, 509, 802
Edwards, S., et al. 2006, ApJ, 646, 319
Gregory, S. G., et al. 2006, MNRAS, 371, 999
Hartmann, L., et al. 1994, ApJ, 426, 669
Kwan, J., et al. 2007, ApJ, 657, 897
Muzerolle, J., et al. 2001, ApJ, 550, 944
Romanova, M. M., et al. 2003, ApJ, 595, 1009